Theory of the Earth

Don L. Anderson

Chapter 3. The Crust and Upper Mantle

Boston: Blackwell Scientific Publications, c1989

Recommended citation:

Anderson, Don L. Theory of the Earth. Boston: Blackwell Scientific Publications, 1989. http://resolver.caltech.edu/CaltechBOOK:1989.001

A scanned image of the entire book may be found at the following persistent URL:

http://resolver.caltech.edu/CaltechBook:1989.001

Abstract:

T he structure of the Earth's interior is fairly well known from seismology, and knowledge of the fine structure is improving continuously. Seismology not only provides the structure, it also provides information about the composition, crystal structure or mineralogy and physical state. In subsequent chapters I will discuss how to combine seismic with other kinds of data to constrain these properties. A recent seismological model of the Earth is shown in Figure 3-1. Earth is conventionally divided into crust, mantle and core, but each of these has subdivisions that are almost as fundamental (Table 3-1). The lower mantle is the largest subdivision, and therefore it dominates any attempt to perform major-element mass balance calculations. The crust is the smallest solid subdivision, but it has an importance far in excess of its relative size because we live on it and extract our resources from it, and, as we shall see, it contains a large fraction of the terrestrial inventory of many elements. In this and the next chapter I discuss each of the major subdivisions, starting with the crust and ending with the inner core.

3

The Crust and Upper Mantle

ZOE: Come and I'll peel off.
BLOOM: (feeling his occiput dubiously with the unparalleled embarrassment of a harassed pedlar gauging the symmetry of her peeled pears) Somebody would be dreadfully jealous if she knew.

—JAMES JOYCE, *ULYSSES*

The structure of the Earth's interior is fairly well known from seismology, and knowledge of the fine structure is improving continuously. Seismology not only provides the structure, it also provides information about the composition, crystal structure or mineralogy and physical state. In subsequent chapters I will discuss how to combine seismic with other kinds of data to constrain these properties. A recent seismological model of the Earth is shown in Figure 3-1. Earth is conventionally divided into crust, mantle and core, but each of these has subdivisions that are almost as fundamental (Table 3-1). The lower mantle is the largest subdivision, and therefore it dominates any attempt to perform major-element mass balance calculations. The crust is the smallest solid subdivision, but it has an importance far in excess of its relative size because we live on it and extract our resources from it, and, as we shall see, it contains a large fraction of the terrestrial inventory of many elements. In this and the next chapter I discuss each of the major subdivisions, starting with the crust and ending with the inner core.

THE CRUST

The major divisions of the Earth's interior—crust, mantle and core—have been known from seismology for about 70 years. These are based on the reflection and refraction of P- and S-waves. The boundary between the crust and mantle is called the Mohorovičić discontinuity (M-discontinuity or Moho for short) after the Croatian seismologist who discovered it in 1909. It separates rocks having P-wave velocities of 6–7 km/s from those having velocities of about 8 km/s. The term "crust" has been used in several ways. It initially referred to the brittle outer shell of the Earth that extended down to the asthenosphere ("weak layer"); this is now called the lithosphere ("rocky layer"). Later it was used to refer to the rocks occurring at or near the surface and acquired a petrological connotation. Crustal rocks have distinctive physical properties that allow the crust to be mapped by a variety of geophysical techniques.

The term "crust" is now used to refer to that region of the Earth above the Moho. It represents 0.4 percent of the Earth's mass. In a strict sense, knowledge of the existence of the crust is based solely on seismological data. The Moho is a sharp seismological boundary and in some regions appears to be laminated. There are three major crustal types—continental, transitional and oceanic. Oceanic crust generally ranges from 5 to 15 km in thickness and comprises 60 percent of the total crust by area and more than 20 percent by volume. In some areas, most notably near oceanic fracture zones, the oceanic crust is as thin as 3 km. Oceanic plateaus and aseismic ridges may have crustal thicknesses greater than 30 km. Some of these appear to represent large volumes of material generated at oceanic spreading centers or hotspots, and a few seem to be continental fragments. Although these anomalously thick crust regions constitute only about 10 percent of the area of the oceans, they may represent up to 50 percent of the total volume of the oceanic crust. Islands, island arcs and continental margins are collectively referred to as transitional crust and generally range from 15 to 30 km in thickness. Continental crust generally ranges from 30 to 50 km thick,

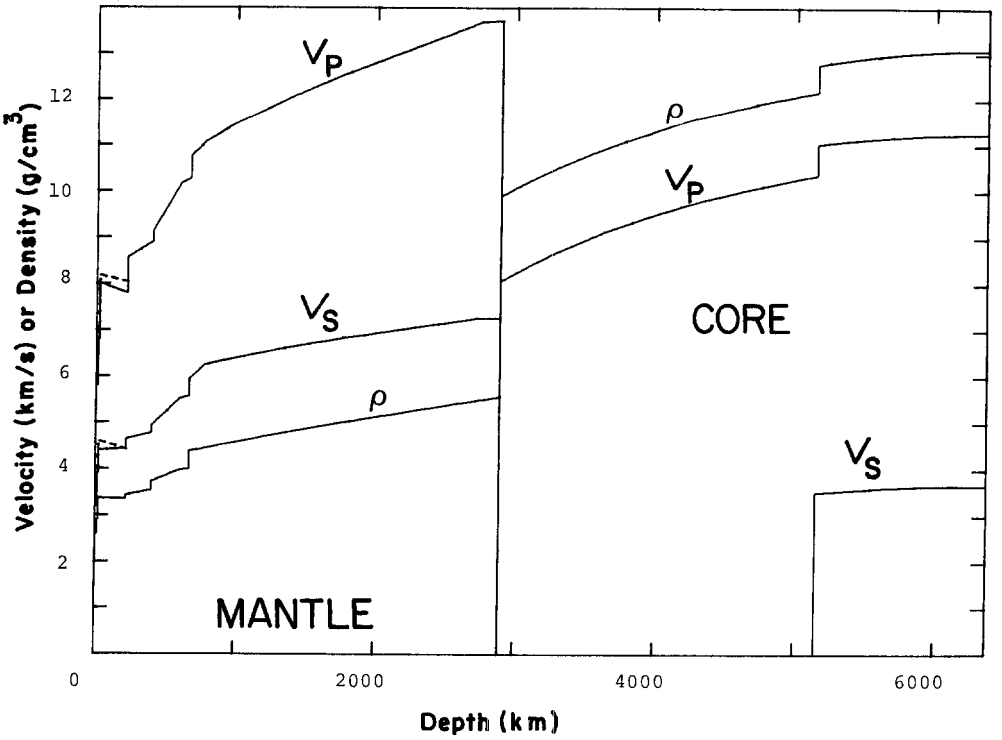

FIGURE 3-1
The Preliminary Reference Earth Model (PREM). The model is anisotropic in the upper 220 km, as shown in Figure 3-3. Dashed lines are the horizontal components of the seismic velocity (after Dziewonski and Anderson, 1981).

but thicknesses up to 80 km are reported in some convergence regions. Based on geological and seismic data, the main rock type in the upper continental crust is granodiorite or tonalite in composition. The lower crust is probably diorite, garnet granulite and amphibolite. The average composition of the continental crust is thought to be similar to andesite or diorite. The upper part of the continental crust is enriched in such "incompatible" elements as potassium, rubidium, barium, uranium and thorium and has a marked negative europium anomaly relative to the mantle. Niobium and tantalum are apparently depleted relative to other normally incompatible trace elements. It has recently been recognized that the terrestrial crust is unusually thin compared to the Moon and Mars and compared to the amount of potential crust in the mantle. This is related to the fact that crustal material converts to dense garnet-rich assemblages at relatively shallow depth. The maximum theoretical thickness of material with crust-like physical properties is about 50–60 km, although the crust may temporarily achieve somewhat greater thickness because of the sluggishness of phase changes at low temperature.

TABLE 3-1
Summary of Earth Structure

Region	Depth (km)	Fraction of Total Earth Mass	Fraction of Mantle and Crust
Continental crust	0–50	0.00374	0.00554
Oceanic crust	0–10	0.00099	0.00147
Upper mantle	10–400	0.103	0.153
Transition region	400–650	0.075	0.111
Lower mantle	650–2890	0.492	0.729
Outer core	2890–5150	0.308	—
Inner core	5150–6370	0.017	—

Clomposition

Mineralogically, feldspar (K-feldspar, plagioclase) is the most abundant mineral in the crust, followed by quartz and hydrous minerals (such as the micas and amphiboles) (Table 3-2). The minerals of the crust and some of their physical properties are given in Table 3-3. **A** crust composed of these minerals will have an average density of about 2.7 g/cm^3. There is enough difference in the velocities and V_p/V_s ratios of the more abundant minerals that seismic velocities provide a good mineralogical discriminant. One uncertainty is the amount of serpentinized ultramafic rocks in the lower crust since serpentinization decreases the velocity of olivine

TABLE 3-2
Crustal Minerals

Mineral	Composition	Range of Crustal Abundances (vol. pct.)
Plagioclase		31–41
Anorthite	$Ca(Al_2Si_2)O_8$	
Albite	$Na(Al,Si_3)O_8$	
Orthoclase		9–21
K-feldspar	$K(Al,Si_3)O_8$	
Quartz	SiO_2	12–24
Amphibole	$NaCa_2(Mg,Fe,Al)_5[(Al,Si)_4O_{11}]_2(OH)_2$	0–6
Biotite	$K(Mg,Fe^{2+})_3(Al,Si_3)O_{10}(OH,F)_2$	4–11
Muscovite	$K\ Al_2(Al,Si_3)O_{10}(OH)$	0–8
Chlorite	$(Mg,Fe^{2+})_5Al(Al,Si_3)O_{10}(OH)_8$	0–3
Pyroxene		
Hypersthene	$(Mg,Fe^{2+})SiO_3$	0–11
Augite	$Ca(Mg,Fe^{2+})(SiO_3)_2$	
Olivine	$(Mg,Fe^{2+})_2SiO_4$	0–3
Oxides		~2
Sphene	$CaTiSiO_5$	
Allanite	$(Ce,Ca,Y)(Al,Fe)_3(SiO_4)_3(OH)$	
Apatite	$Ca_5(PO_4,CO_3)_3(F,OH,Cl)$	
Magnetite	$FeFe_2O_4$	
Ilmenite	$FeTiO_3$	

to crustal values. In some regions the seismic Moho may not be at the base of the basaltic section but at the base of the serpentinized zone in the mantle.

Estimates of the composition of the oceanic and continental crust are given in Table 3-4; another that covers the trace elements is given in Table 3-5. Note that the continental crust is richer in SiO_2, TiO_2, Al_2O_3, Na_2O and K_2O than the oceanic crust. This means that the continental crust is richer in quartz and feldspar and is therefore intrinsically less dense than the oceanic crust. The mantle under stable continental-shield crust has seismic properties that suggest that it is intrinsically less dense than mantle elsewhere. The elevation of continents is controlled primarily by the density and thickness of the crust and the intrinsic density and temperature of the underlying mantle. It is commonly assumed that the seismic Moho is also the petrological Moho, the boundary between sialic or mafic crustal rocks and ultramafic mantle rocks. However, partial melting, high pore pressure and serpentinization can reduce the velocity of mantle rocks, and increased abundances of olivine and pyroxene can increase the velocity of crustal rocks. High pressure also increases the velocity of mafic rocks, by the gabbro-eclogite phase change, to mantle-like values. The increase in velocity from "crustal" to "mantle" values in regions of thick continental crust may be due, at least in part, to the appearance of garnet as a stable phase. The situation is complicated further by kinetic considerations. Garnet is a common metastable phase in near-surface intrusions such as pegmatites and metamorphic teranes. On the other hand, feldspar-rich rocks may exist at depths greater than the gabbro-eclogite equilibrium boundary if temperatures are so low that the reaction is sluggish.

The common assumption that the Moho is a chemical boundary is in contrast to the position commonly taken with regard to other mantle discontinuities. It is almost univer-

TABLE 3-3
Average Crustal Abundance, Density and Seismic Velocities of Major Crustal Minerals

Mineral	Volume percent	ρ (g/cm^3)	V_p (km/s)	V_s (km/s)
Quartz	12	2.65	6.05	4.09
K-feldspar	12	2.57	5.88	3.05
Plagioclase	39	2.64	6.30	3.44
Micas	5	2.8	5.6	2.9
Amphiboles	5	3.2	7.0	3.8
Pyroxene	11	3.3	7.8	4.6
Olivine	3	3.3	8.4	4.9

TABLE 3-4
Estimates of the Chemical Composition of the Crust (Weight Percent)

Oxide	Oceanic Crust	Continental Crust	
	(1)	(2)	(3)
SiO_2	47.8	63.3	58.0
TiO_2	0.59	0.6	0.8
Al_2O_3	12.1	16.0	18.0
Fe_2O_3	—	1.5	—
FeO	9.0	3.5	7.5
MgO	17.8	2.2	3.5
CaO	11.2	4.1	7.5
Na_2O	1.31	3.7	3.5
K_2O	0.03	2.9	1.5
H_2O	1.0	0.9	—

(1) Elthon (1979).
(2) Condie (1982).
(3) Tayor and McLennan (1985).

sally assumed that the major mantle discontinuities represent equilibrium solid-solid phase changes in a homogeneous material. It should be kept in mind that chemical changes may also occur in the mantle. It is hard to imagine how the Earth could have gone through a high-temperature accretion and differentiation process and maintained a homogeneous composition throughout. It is probably not a coincidence that the maximum crustal thicknesses are close to the basalt-eclogite boundary. Eclogite is denser than peridotite, at least in the shallow mantle, and will tend to fall into normal mantle, thereby turning a phase boundary (basalt-eclogite) into a chemical boundary (basalt-peridotite).

Seismic Velocities in the Crust and Upper Mantle

Seismic velocities in the crust and upper mantle are typically determined by measuring the transit time between an earthquake or explosion and an array of seismometers. Crustal compressional wave velocities in continents, beneath the sedimentary layers, vary from about *5* km/s at shallow depth to about 7 km/s at a depth of *30* to *50* km. The lower velocities reflect the presence of pores and cracks more than the intrinsic velocities of the rocks. At greater depths the pressure closes cracks and the remaining pores are fluid-saturated. These effects cause a considerable increase in velocity. A typical crustal velocity range at depths greater than 1 km is 6–7 km/s. The corresponding range in shear velocity is about *3.5* to 4.0 km/s. Shear velocities can be determined from both body waves and the dispersion of short-period surface waves. The top of the mantle under

TABLE 3-5
Composition of the Bulk Continental Crust, by Weight

SiO_2	57.3 pct.	Co	29 ppm	Ce	33 ppm
TiO_2	0.9 pct.	Ni	105 ppm	Pr	3.9 ppm
Al_2O_3	15.9 pct.	Cu	75 ppm	Nd	16 ppm
FeO	9.1 pct.	Zn	80 ppm	Sm	3.5 ppm
MgO	5.3 pct.	Ga	18 ppm	Eu	1.1 ppm
CaO	7.4 pct.	Ge	1.6 ppm	Gd	3.3 ppm
Na_2O	3.1 pct.	As	1.0 ppm	Tb	0.6 ppm
K_2O	1.1 pct.	Se	0.05 ppm	Dy	3.7 ppm
Li	13 ppm	Rb	32 ppm	Ho	0.78 ppm
Be	1.5 ppm	Sr	260 ppm	Er	2.2 ppm
B	10 ppm	Y	20 ppm	Tm	0.32 ppm
Na	2.3 pct.	Zr	100 ppm	Yb	2.2 ppm
Mg	3.2 pct.	Nb	11 ppm	Lu	0.30 ppm
Al	8.41 pct.	Mo	1 ppm	Hf	3.0 ppm
Si	26.77 pct.	Pd	1 ppb	Ta	1 ppm
K	0.91 pct.	Ag	80 ppb	W	1 ppm
Ca	5.29 pct.	Cd	98 ppb	Re	0.5 ppb
Sc	30 ppm	In	50 ppb	Ir	0.1 ppb
Ti	5400 ppm	Sn	2.5 ppm	Au	3 ppb
V	230 ppm	Sb	0.2 ppm	Tl	360 ppb
Cr	185 ppm	Cs	1 ppm	Pb	8 ppb
Mn	1400 ppm	Ba	250 ppm	Bi	60 ppb
Fe	7.07 pct.	La	16 ppm	Th	3.5 ppm
				U	0.91 ppm

Taylor and McLennan (1985).

continents usually has velocities in the range 8.0 to 8.2 km/s for compressional waves and 4.3 and 4.7 km/s for shear waves.

The compressional velocity near the base of the oceanic crust usually falls in the range 6.5–6.9 kmls. In some areas a thin layer at the base of the crust with velocities as high as 7.5 km/s has been identified. The oceanic upper mantle has a P-velocity (P_n) that varies from about 7.9 to 8.6 km/s. The velocity increases with oceanic age, because of cooling, and varies with azimuth, presumably due to crystal orientation. The fast direction is generally close to the inferred spreading direction. The average velocity is close to 8.2 km/s, but young ocean has velocities as low as 7.6 km/s. Tectonic regions also have low velocities.

Since water does not transmit shear waves and since most velocity measurements use explosive sources, it is difficult to measure the shear velocity in the oceanic crust and upper mantle. There are therefore fewer measurements of shear velocity, and these have higher uncertainty and lower resolution than those for P-waves. The shear velocity increases from about 3.6–3.9 to 4.4–4.7 km/s from the base of the crust to the top of the mantle.

Ophiolite sections found at some continental margins are thought to represent upthrust or obducted slices of the oceanic crust and upper mantle. These sections grade downward from pillow lavas to sheeted dike swarms, intrusives, pyroxene and olivine gabbro, layered gabbro and peridotite and, finally, harzburgite and dunite. Laboratory velocities in these rocks are given in Table 3-6. There is good agreement between these velocities and those actually observed in the oceanic crust and upper mantle. The sequence of extrusive~intrusives and cumulates is consistent with what is expected at a midocean-ridge magma chamber. Many ophiolites apparently represent oceanic crust formed near island arcs in marginal basins. They might not be typical of crustal sections formed at mature midoceanic spreading centers. Marginal basin basalts, however, are very similar to mid-ocean-ridge basalts, at least in major-element chemistry, and the bathymetry, heat flow and seismic crustal structure in marginal basins are similar to values for the major ocean basins.

The velocity contrast between the lower crust and upper mantle is commonly smaller beneath young orogenic areas (0.5 to 1.5 km/s) than beneath cratons and shields (1 to 2 kmls). Continental rift systems have thin crust (less than 30 km) and low P_n velocities (less than 7.8 kmls). Thinning of the crust in these regions appears to take place by thinning of the lower crust. In island arcs the crustal thickness ranges from about 5 km to 35 km. In areas of very thick crust such as in the Andes (70 km) and the Himalayas (80 km), the thickening occurs primarily in the lower crustal layers. Paleozoic orogenic areas have about the same range of crustal thicknesses and velocities as platform areas.

TABLE 3-6
Density, Compressional Velocity and Shear Velocity in Rock Types Found in Ophiolite Sections

Rock Type	ρ (g/cm^3)	V_p (km/s)	V_s (km/s)	Poisson's Ratio
Metabasalt	2.87	6.20	3.28	0.31
Metadolerite	2.93	6.73	3.78	0.27
Metagabbro	2.95	6.56	3.64	0.28
Gabbro	2.86	6.94	3.69	0.30
Pyroxenite	3.23	7.64	4.43	0.25
Olivine gabbro	3.30	7.30	3.85	0.32
Harzburgite	3.30	8.40	4.90	0.24
Dunite	3.30	8.45	4.90	0.25

Salisbury and Christensen (1978), Christensen and Smewing (1981).

THE SEISMIC LITHOSPHERE OR LID

Uppermost mantle velocities are typically 8.0 to 8.2 kmls, and the spread is about 7.9–8.6 kmls. Some long refraction profiles give evidence for a deeper layer in the lithosphere having a velocity of 8.6 km/s. The seismic lithosphere, or LID, appears to contain at least two layers. Long refraction profiles on continents have been interpreted in terms of a laminated model of the upper 100 km with high-velocity layers, 8.6–8.7 km/s or higher, embedded in "normal" material (Fuchs, 1977). Corrected to normal conditions these velocities would be about 8.9–9.0 kmls. The P-wave gradients are often much steeper than can be explained by self-compression. These high velocities require oriented olivine or large amounts of garnet. The detection of 7–8 percent azimuthal anisotropy for both continents and oceans suggests that the shallow mantle at least contains oriented olivine. Substantial anisotropy is inferred to depths of at least 50 km depth in Germany (Bamford, 1977).

The average values of V_p and V_s at 40 km when corrected to standard conditions are 8.72 kmls and 4.99 km/s, respectively. The corrections for temperature amount to 0.5 and 0.3 km/s, respectively, for V_p and V_s. The pressure corrections are much smaller. Short-period surface wave data have better resolving power for V_s in the LID. Applying the same corrections to surface wave data (Morris and others, 1969), we obtain 4.48–4.55 km/s and 4.51–4.64 km/s for 5-Ma-old and 25-Ma-old oceanic lithosphere. Presumably, velocities can be expected to increase further for older regions. A value for V_p of 8.6 km/s is commonly observed near 40 km depth in the oceans. This corresponds to about 8.87 km/s at standard conditions. These values can be compared with 8.48 and 4.93 kmls for olivine-rich aggregates. Eclogites have V_p and V_s as high as 8.8 and 4.9 kmls in certain directions and as high as 8.61 and 4.86 kmls as average values.

All of the above suggests that corrected velocities of at least 8.6 and 4.8 km/s, for V_p and V_s, respectively, occur in

the lower lithosphere, and this requires substantial amounts of garnet at relatively shallow depths. At least 26 percent garnet is required to satisfy the compressional velocities. The density of such an assemblage is about 3.4 g/cm³. If one is to honor the higher seismic velocities, even greater proportions of garnet are required. The lower lithosphere may therefore be gravitationally unstable with respect to the underlying mantle, particularly in oceanic regions. The upper mantle under shield regions is consistent with a very olivine-rich peridotite which is buoyant and therefore stable relative to "normal" mantle.

Most refraction profiles, particularly at sea, sample only the uppermost lithosphere. P_n velocities of 8.0–8.2 km/s are consistent with peridotite or harzburgite, thought by some to be the refractory residual after basalt removal. Anisotropies are also appropriate for olivine-pyroxene assemblages. The sequence of layers, at least in oceanic regions, seems to be basalt, peridotite, eclogite.

Anisotropy of the upper mantle is a potentially useful petrological constraint, although it can also be caused by organized heterogeneity, such as laminations or parallel dikes and sills or aligned partial melt zones, and stress fields. Under oceans the uppermost mantle, the P_n region, exhibits an anisotropy of 7 percent (Morris and others, 1969). The fast direction is in the direction of spreading, and the magnitude of the anisotropy and the high velocities of P_n arrivals suggest that oriented olivine crystals control the elastic properties. Pyroxene exhibits a similar anisotropy, whereas garnet is more isotropic. The preferred orientation is presumably due to the emplacement or freezing mechanism, the temperature gradient or to nonhydrostatic stresses. A peridotite layer at the top of the oceanic mantle is consistent with the observations.

The average anisotropy of the upper mantle is much less than the values given above. Forsyth (1975) studied the dispersion of surface waves and found shear-wave anisotropies, averaged over the upper mantle, of 2 perent. Shear velocities in the LID vary from 4.26 to 4.46 km/s, increasing with age; the higher values correspond to a lithosphere 10–50 Ma old. This can be compared with shear-wave velocities of 4.30–4.86 km/s and anisotropies of 1–4.7 percent found in relatively unaltered eclogites (Manghnani, et al, 1974). The compressional velocity range in the same samples is 7.90–8.61 km/s, reflecting the large amounts of garnet. Surface waves exhibit both azimuthal and polarization anisotropy for at least the upper 200 km of the mantle.

On the basis of data available at the time, Ringwood suggested in 1975 that the V_p/V_s ratio of the lithosphere was smaller than measured on eclogites. He therefore ruled out eclogite as an important constituent of the lithosphere. The eclogite-peridotite controversy regarding the composition of the suboceanic mantle is long standing and still unresolved. Newer and more complete data on the V_p/V_s ratio in eclogites show that the high-V_p/V_s eclogites are generally of low density and contain plagioclase or olivine. The higher-density eclogites are consistent with the properties of the lower lithosphere. Garnet and clinopyroxene may be important components of the lithosphere. A lithosphere composed primarily of olivine and $(Mg,Fe)SiO_3$, that is, pyrolite or lherzolite, does not satisfy the seismic data for the bulk of the lithosphere. The lithosphere, therefore, is not just cold mantle, or a thermal boundary layer alone.

Oceanic crustal basalts represent only part of the basaltic fraction of the upper mantle. The peridotite layer represents depleted mantle or refractory cumulates but may be of any age. Basaltic material may also be intruded at depth. It is likely that the upper mantle is layered, with the volatiles and melt products concentrated toward its top. As the lithosphere cools, this basaltic material is incorporated onto the base of the plate, and as the plate thickens it eventually transforms to eclogite, yielding high velocities and increasing the thickness and mean density of the oceanic plate. Eventually the plate becomes denser than the underlying asthenosphere, and conditions become appropriate for subduction or delamination.

O'Hara (1968) argued that erupted lavas are not the original liquids produced by partial melting of the upper mantle, but are residual liquids from processes that have left behind complementary eclogite accumulates in the upper mantle. Such a model is consistent with the seismic obser-

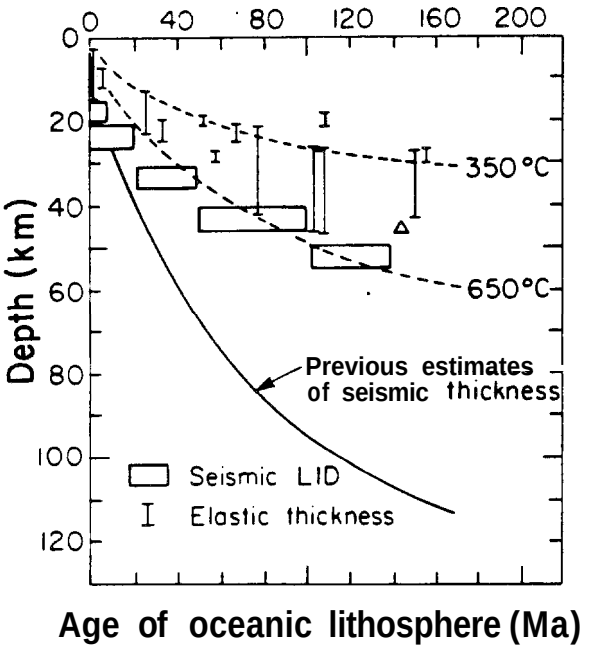

FIGURE 3-2
The thickness of the lithosphere as determined from flexural loading studies and surface waves. The upper edges of the open boxes gives the thickness of the seismic LID (high-velocity layer, or seismic lithosphere). The lower edge gives the thickness of the mantle LID plus the oceanic crust (Regan and Anderson, 1984). The triangle is a refraction measurement of oceanic seismic lithosphere thickness (Shimamura and others, 1977). The LID under continental shields is about 150 km thick (see Figure 3-4).
thick (see Figure 3-4).

vations of high velocities for P_n at midlithospheric depths and with the propensity of oceanic lithosphere to plunge into the asthenosphere. The latter observation suggests that the average density of the lithosphere is greater than that of the asthenosphere.

The thickness of the seismic lithosphere, or high-velocity LID, is about 150 km under continental shields. Some surface-wave results give a much greater thickness. A thin low-velocity zone (LVZ) at depth, as found from body-wave studies, however, cannot be well resolved with long-period surface waves. The velocity reversal between about 150 and 200 km in shield areas is about the depth inferred for kimberlite genesis, and the two phenomena may be related.

There is very little information about the deep oceanic lithosphere from body-wave data. Surface waves have been used to infer a thickening with age of the oceanic lithosphere to depths greater than 100 km (Figure 3-2). However, when anisotropy is taken into account, the thickness may be only about 50 km for old oceanic lithosphere (Regan and Anderson, 1984). This is about the thickness inferred for the "elastic" lithosphere from flexural bending studies around oceanic islands and at trenches.

The seismic velocities of some upper-mantle minerals and rocks are given in Tables 3-7 and 3-8, respectively. Garnet and jadeite have the highest velocities, clinopyroxene and orthopyroxene the lowest. Mixtures of olivine and orthopyroxene (the peridotite assemblage) can have velocities similar to mixtures of garnet-diopside-jadeite (the eclogite assemblage). Garnet-rich assemblages, however, have velocities higher than orthopyroxene-rich assemblages. The V_p/V_s ratio is greater for the eclogite minerals than for the peridotite minerals. This ratio plus the anisotropy are useful diagnostics of mantle mineralogy. High velocities alone do not necessarily discriminate between garnet-rich and olivine-rich assemblages. Olivine is very anisotropic, having compressional velocities of 9.89, 8.43 and 7.72 km/s along the principal crystallographic axes. Orthopyroxene, likewise, has velocities ranging from 6.92 to 8.25 km/s, depending on direction. In natural olivine-rich aggregates (Table 3-9), the maximum velocities are about 8.7 and 5.0 km/s for P-waves and S-waves, respectively. With 50 percent orthopyroxene the velocities are reduced to 8.2 and 4.85 km/s, and the composite is nearly isotropic. Eclogites are also nearly isotropic.

The "standard model" for the oceanic lithosphere assumes 24 km of depleted peridotite, complementary to and contemporaneous with the basaltic crust, between the crust and the presumed fertile peridotite upper mantle. There is no direct evidence for this hypothetical model. The lower oceanic lithosphere may be much more basaltic or eclogitic than in this simple model.

TABLE 3-7
Densities and Elastic-wave Velocities in Upper-mantle Minerals

Mineral	ρ (g/cm^3)	V_p	V_s (km/s)	V_p/V_s
Olivine				
Fo	3.214	8.57	5.02	1.71
Fo_{93}	3.311	8.42	4.89	1.72
Fa	4.393	6.64	3.49	1.90
Pyroxene				
En	3.21	8.08	4.87	1.66
En_{80}	3.354	7.80	4.73	1.65
Fs	3.99	6.90	3.72	1.85
Di	3.29	7.84	4.51	1.74
Jd	3.32	8.76	5.03	1.74
Garnet				
Py	3.559	8.96	5.05	1.77
Al	4.32	8.42	4.68	1.80
Gr	3.595	9.31	5.43	1.71
Kn	3.85	8.50	4.79	1.77
An	3.836	8.51	4.85	1.75
Uv	3.85	8.60	4.89	1.76

Sumino and Anderson (1984).

TABLE 3-8
Densities and Elastic-wave Velocities of Upper-mantle Rocks

Rock	ρ	V_p	V_s	V_p/V_s
Garnet	3.53	8.29	4.83	1.72
lherzolite	3.47	8.19	4.72	1.74
	3.46	8.34	4.81	1.73
	3.31	8.30	4.87	1.70
Dunite	3.26	8.00	4.54	1.76
	3.31	8.38	4.84	1.73
Bronzitite	3.29	7.89	4.59	1.72
	3.29	7.83	4.66	1.68
Eclogite	3.46	8.61	4.77	1.81
	3.61	8.43	4.69	1.80
	3.60	8.42	4.86	1.73
	3.55	8.22	4.75	1.73
	3.52	8.29	4.49	1.85
	3.47	8.22	4.63	1.78
Jadeite	3.20	8.28	4.82	1.72

Clark (1966), Babuska (1972), Manghnani and others (1974), Jordan (1979).

THE LOW-VELOCITY ZONE OR LVZ

A region of diminished velocity or negative velocity gradient in the upper mantle was proposed by Beno Gutenberg in 1959. Earlier, just after isostasy had been established, it had been concluded that a weak region underlay the relatively strong lithosphere. This has been called the asthenosphere. The discovery of a low-velocity zone strengthened

TABLE 3-9
Anisotropy of Upper-mantle Rocks

Mineralogy	Direction	V_p	V_{s_1}	V_{s_2}	V_p/V_s	
			Peridotites			
100 pct. ol	I	8.7	5.0	4.85	1.74	1.79
	2	8.4	4.95	4.70	1.70	1.79
	3	8.2	4.95	4.72	1.66	1.74
70 pct. ol,	1	8.4	4.9	4.77	1.71	1.76
30 pct. opx	2	8.2	4.9	4.70	1.67	1.74
	3	8.1	4.9	4.72	1.65	1.72
100 pct. opx	1	7.8	4.75	4.65	1.64	1.68
	2	7.75	4.75	4.65	1.63	1.67
	3	7.78	4.75	4.65	1.67	1.67
			Eclogites			
51 pct. ga,	1	8.476		4.70		1.80
23 pct. cpx,	2	8.429		4.65		1.81
24 pct. opx	3	8.375		4.71		1.78
47 pct. ga,	1	8.582		4.91		1.75
45 pct. cpx	2	8.379		4.87		1.72
	3	8.30		4.79		1.73
46 pct. ga,	1	8.31		4.77		1.74
37 pct. cpx	2	8.27		4.77		1.73
	3	8.11		4.72		1.72

Manghnani and others (1974), Christensen and Lundquist (1982).

the concept of an asthenosphere, even though a weak layer is not necessarily a low-velocity layer.

Gutenberg based his conclusions primarily on amplitudes and apparent velocities of waves from earthquakes in the vicinity of the low-velocity zone. He found that at distances from about 1° to 15° the amplitudes of longitudinal waves decrease about exponentially with distance. At 15" they increase suddenly by a factor of more than 10 and then decrease at greater distances. These results can be explained in terms of a low-velocity region, which defocuses seismic energy, underlain by a higher gradient that serves to focus the rays.

Most recent models of the velocity distribution in the upper mantle include a region of high gradient between 250 and 350 km depth. Lehmann (1961) interpreted her results for several regions in terms of a discontinuity at 220 km (sometimes called the Lehmann discontinuity), and many subsequent studies give high-velocity gradients near this depth.

It is difficult to study details of the velocity distribution in and just below a low-velocity zone, and it is still not clear if the base of'the low-velocity zone is gradual or abrupt. Reflections have been reported from depths between 190 and 250 km by a number of authors (Anderson, 1979). This situation is further complicated by the extreme lateral heterogeneity of the upper 200 km of the mantle. This region is also low Q (high attenuation) and anisotropic. Some recent results are shown in Figures 3-3 and 3-4.

Various interpretations have been offered for the low-velocity zone. This is undoubtedly a region of high thermal gradient, the boundary layer between the near surface where heat is transported by conduction and the deep interior where heat is transported by convection. If the temperature gradient is high enough, the effects of pressure can be overcome and velocity can decrease with depth. It can be shown, however, that a high temperature gradient alone is not an adequate explanation. Partial melting and dislocation

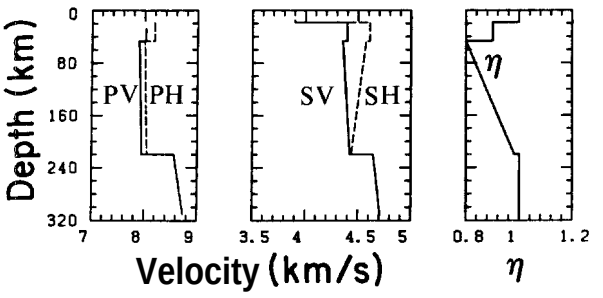

FIGURE **3-3**
Velocity-depth profiles for the average Earth, as determined from surface waves (Regan and Anderson, 1984). From left to right, the graphs show P-wave velocities (vertical and horizontal), S-wave velocities (vertical and horizontal), and the anisotropy parameter η (see Chapter 15), where 1 represents isotropy.

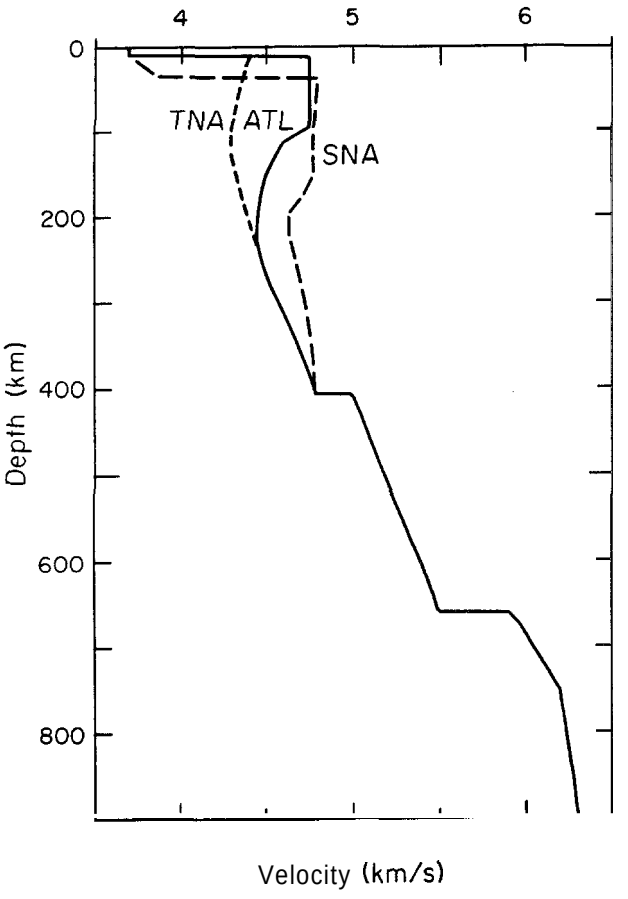

FIGURE 3-4
High-resolution shear-wave velocity profiles for various tectonic provinces; TNA is tectonic North America, SNA is shield North America, ATL is north Atlantic (after Grand and Helmberger, 1984).

relaxation both cause a large decrease in velocity. For partial melting to be effective the melt must occur, microscopically, as thin grain boundary films or, macroscopically, as narrow dikes or sills. Melting experiments suggest that melting occurs at grain corners and is more likely to occur in interconnected tubes. This also seems to be required by electrical conductivity data. However, numerous thin dikes and sills act macroscopically as thin films for long-wavelength seismic waves. High attenuation is associated with relaxation processes such as grain boundary relaxation, including partial melting, and dislocation relaxation. Allowance for anelastic dispersion increases the velocities in the low-velocity zone determined by free-oscillation and surface-wave techniques (Hart and others, 1976), but partial melting is still required to explain the regions of very low velocity. Allowance for anisotropy results in a further upward revision for the velocities in this region (Dziewonski and Anderson, 1981), as discussed below. This plus the recognition that subsolidus effects, such as dislocation relaxation, can cause a substantial decrease in velocity has complicated the interpretation of seismic velocities in the shallow mantle. Velocities in tectonic regions and under some oceanic regions, however, are so low that partial melting is implied. In most other regions a subsolidus mantle composed of oriented olivine-rich aggregates can explain the velocities and anisotropies to depths of about 200 km. There is, as yet, no detailed information on anisotropy below 220 km in any single geographic region. The global inversions of Nataf and others **(1986)** involve a laterally heterogeneous velocity and anisotropy structure to depths as great as 400 km, but anisotropy resolution below 200 km is poor.

The rapid increase in velocity below 220 km may be due to chemical or compositional changes or to transition from relaxed to unrelaxed moduli. The latter explanation will involve an increase in Q, and some Q models exhibit this characteristic. However, the resolving power for Q is low, and most of the seismic Q data can be satisfied with a constant-Q upper mantle, at least down to 400 km.

The low-velocity zone is very thin under shields, extending from about 150 to 200 km. Under the East Pacific Rise low velocities persist to 400 km, and the Lehmann discontinuity appears to be absent. One possible interpretation is that material from below 200 km rises to the near surface under ridges, thereby breaking through any chemical discontinuity. The fact that earthquakes associated with subduction of young oceanic lithosphere do not extend below 200 km suggests that this may be a buoyancy, or chemical, discontinuity. Old dense lithosphere, however, penetrates deeper.

The velocities between 200 and 400 km can be satisfied by either an olivine-rich aggregate, such as peridotite, or a garnet-clinopyroxene aggregate such as eclogite. Deep seated kimberlites bring xenoliths of both types to the surface, although the eclogite nodules are much rarer. Oceanic ridges have low velocities throughout this depth range, suggesting that the source region for midocean ridge basalts is in the transition region (middle mantle) rather than in the low-velocity zone. Many petrologists assume that the low-velocity zone is the source region for most basalts. This is based on early seismological interpretations of a global layer of partial melt at that depth. Basalts from a deeper layer must, of course, traverse the low-velocity zone, and this is probably where melt-crystal separation occurs and where increased melting due to adiabatic ascent occurs. Under the East Pacific Rise the maximum V_p/V_s ratio occurs at about 100 km, and that is where melting caused by adiabatic ascent from deeper levels is most pronounced in this region and probably other ridges as well.

Recent surface-wave tomographic results show that the lateral variations of velocity in the upper mantle are as pronounced as the velocity variations that occur with depth (Nataf and others, **1986).** Thus, it is misleading to think of the mantle as a simple layered system. Below 400 km there

is little evidence from body waves for large lateral variations. Detailed body-wave modeling for regions as diverse as the Canadian and Baltic shields, western North America–East Pacific Rise, northwestern North America and the western Atlantic, while exhibiting large changes above 200 km, converge from 200 to 400 km. Surface waves have detected small lateral changes between depths of 400 and 650 km. Lateral changes are, of course, expected in a convecting mantle because of variations in temperature and anisotropy due to crystal orientation.

The geophysical data (seismic velocities, attenuation, heat flow) can be explained if the low-velocity regions in the shallow mantle are permeated by partial melt (Anderson and Sammis, 1970; Anderson and Bass, 1984). This explanation, in turn, suggests the presence of volatiles in order to depress the solidus of mantle materials, or a high-temperature mantle. The top of the low-velocity zone may mark the crossing of the geotherm with the wet solidus of peridotite. Its termination would be due to (1) a crossing in the opposite sense of the geotherm and the solidus, (2) the absence of water or other volatiles, or **(3)** the removal of water into high-pressure hydrous or hydroxylated phases. In all of these cases the boundaries of the low-velocity zone would be expected to be sharp. Small amounts of melt (about 1 percent) can explain the velocity reduction if the melt occurs as thin grain-boundary films. Considering the wavelength of seismic waves, magma-filled dikes and sills, rather than intergranular melt films, would also serve to decrease the seismic velocity by the appropriate amount.

The melting that is inferred for the lower velocity regions of the upper mantle may be initiated by adiabatic ascent from deeper levels. The high compressibility and high iron content of melts means that the density difference between melts and residual crystals decreases with depth. High temperatures and partial melting tend to decrease the garnet content and thus to lower the density of the mantle. Buoyant diapirs from depths greater than 200 km will extensively melt on their way to the shallow mantle. Therefore, partially molten material as well as melts can be delivered to the shallow mantle. The ultimate source of basaltic melts may be below 300–400 km even if melt-solid separation does not occur until shallower depths.

The Base of the LVZ

The major seismic discontinuities in the mantle are near 400 and 670 km, bracketing the transition region. There is another important region of high velocity gradient at a depth near 220 km, the base of the low-velocity zone. A discontinuity at 232 km depth was proposed in 1917 by Galitzin. The most detailed early studies, by Inge Lehmann (1961), indicated the presence of a discontinuity under North America and Europe near 215–220 km, and this is sometimes referred to as the Lehmann discontinuity. This is confusing since the outer core–inner core boundary is also sometimes given this name.

Many recent studies have found evidence for a discontinuity or high-gradient region between 190 and 230 km from body-wave data (Drummond and others, 1982). The increase in velocity is on the order of 3.5–4.5 percent. Niazi (1969) demonstrated that the Lehmann discontinuity in California and Nevada is a strong reflector and found a depth of 227 ± 22 km. Reflectors at 140–160 km depth may represent an upwarping of the Lehmann discontinuity caused by hotter than normal mantle.

Converted phases have been reported from a discontinuity at a depth of 200–250 km under the Canadian and Baltic shields (Jordan and Frazer, 1975; Sacks and others, 1977). Reflections from a similar depth have been reported from P′P′ precursors for Siberia, western Europe, North Atlantic, Atlantic-Indian Rise, Antarctica, and the Ninety-east Ridge (Whitcomb and Anderson, 1970). Evidence now exists for the Lehmann discontinuity in the eastern and western United States, Canadian Shield, Baltic Shield, oceanic ridges, normal ocean, Australia, the Hindu Kush, the Alps, and the African rift. The V_p/V_s ratio of recent Earth models reverses trend near 220 km. This is indicative of a change in composition, phase, or temperature gradient.

There is a variety of indirect evidence in support of an important boundary near 220 km. This boundary affects seismicity and may be a density or mechanical impediment to slab penetration. It marks the depth above which there are large differences between continental shields and oceans. Few earthquakes occur below this depth in continental collision zones and in regions where the subducting lithosphere is less than about 50 Ma old. In most seismic regions, earthquakes do not occur deeper than about 250 km. This applies to oceanic, continental, and mixed domains. The maximum depths are 200 km in the South Sandwich arc, Burma, Rumania, the Hellenic arc, and the Aleutian arc; 250 km in the west Indian arc; and 300 km in the Ryukyu arc and the Hindu Kush. There are large gaps in seismicity between 250 km and 500–650 km in New Zealand, New Britain, Mindanao, Sunda, New Hebrides, Kuriles, North Chile, Peru, South Tonga, and the Marianas. In the New Hebrides there is a concentration of seismic activity between 190 and 280 km that moves up to 110 and 150 km in the region where a buoyant ridge is attempting to subduct. In the Bonin-Mariana region there is an increase in activity at 280–340 km to the south and a general decrease in activity with depth down to about 230 km. In the Tonga-Kermadec region, seismic activity decreases rapidly down to 230 km and, in the Tonga region, picks up again at 400 km. In Peru most of the seismicity occurs above 190–230 km, and there is a pronounced gap between this depth and 500 km. In Chile the activity is confined to above 230 km and below 500 km. Cross sections of seismicity in these regions suggest impediments to slab penetration at

depths of about 230 and 600 km. Oceanic lithosphere with buoyant ridges appears to penetrate only to 150 km.

Compressional stresses parallel to the dip of the seismic zone are prevalent everywhere that the zone exists below about 300 km, indicating resistance to downward motion below about this depth (Isacks and Molnar, 1971). Actually, between 200 and 300 km about half the focal mechanisms indicate downdip compression, and most of the mechanisms below 215 km are compressional, suggesting that the slabs encounter stronger or denser material that resists their sinking. Resistance at a much deeper level, however, may also explain the seismicity.

In the regions of continent-continent collision, the distribution of earthquakes should define the shape and depth of the collision zone. The Hindu Kush is characterized by a seismicity pattern terminating in an active zone at 215 km. A pronounced minimum in seismic activity occurs at 160 km.

The most conclusive body-wave evidence for the Lehmann discontinuity comes from the study of earthquakes near this depth (Hales and others, 1980). These studies determine a velocity contrast of 0.2 to 0.3 km/s. If the contrast is truly sharp, a chemical discontinuity may occur, at least locally. Compressional velocities in garnet lherzolite, a rock type thought to make up the shallow mantle, are typically 8.2 to 8.3 km/s under normal conditions. These rocks are generally anisotropic with directional velocities ranging from about 8.1 to 8.4 km/s. Natural eclogites have V_p velocities in the range 8.22 to 8.61 km/s. Natural garnets have velocities of the order of 8.8 to 9.0 km/s; jadeite, a component of eclogite clinopyroxenes, has V_p of 8.7 km/s. A garnet- and clinopyroxene-rich eclogite can therefore have extremely high velocities. Therefore, a transition from garnet lherzolite to eclogite would give a seismic discontinuity. Because of the low melting point of garnet and clinopyroxene and the rapid decrease in density of garnet-clinopyroxene aggregates as the pressure is decreased or the temperature increased, a deep eclogite layer is potentially unstable. At low temperature eclogite is denser than lherzolite, but as the temperature rises it can become less dense and an instability will develop. In high-temperature regions of the mantle, the discontinuity may be destroyed.

The V_p/V_s ratios for lherzolites are generally lower (1.73) than for eclogites (-1.8). This is another possible diagnostic and suggests that the shear-wave velocity jump associated with such a chemical discontinuity will be less than the jump in V_p.

In Australia the Lehmann discontinuity is underlain by a low-velocity zone that has a gradual onset about 30 km below the discontinuity. Leven and others (1981) suggested that the velocity knee represents a zone of decoupling of the continental lithosphere from the deeper mantle and that the high velocities result from anisotropy due to alignment of olivine crystals along the zone of movement. They argued that a lherzolite-eclogite chemical change could not explain the high-velocity contrast, but they used theoretical estimates of velocity in lherzolite and measured values on natural eclogites and discarded the higher eclogite values. Natural rocks have lower velocities than theoretical aggregates made out of the same minerals because of the effects of pores and cracks.

The Lehmann discontinuity is enigmatic—it is difficult to observe with surface-focus events and is apparently not present in some areas. In contrast to most other seismic discontinuities, the waves refracted from the Lehmann discontinuity generally do not form first arrivals. Reflections and arrivals from intermediate-focus earthquakes are therefore the best sources of data. If there is a layer of eclogite in the upper mantle, it should show up as a discontinuity in P-wave velocities but may not appear in S-wave profiles because of the change in V_p/V_s. The discontinuity also may not show up at all azimuths because, in certain directions, olivine-rich aggregates can be faster than eclogite. I will show, later in this chapter, that the 400-km discontinuity may, on average, separate olivine-rich peridotite from a more eclogite-rich transition region. In the hotter parts of the mantle, the eclogite-rich layer may rise into the shallow mantle, generating midocean-ridge basalts.

Effect of Anisotropy on the LVZ

The pronounced minimum in the group velocity of long-period mantle Rayleigh waves is one of the classic arguments for the presence of an upper-mantle low-velocity zone. This argument, however, is invalid if the upper mantle is anisotropic (Anderson, 1966; Dziewonski and Anderson, 1981; Anderson and Dziewonski, 1982). The most recent dispersion data can be satisfied with anisotropic models that have only modest gradients in seismic velocities in the upper 200 km of the mantle (Anderson and Dziewonski, 1982). These models differ considerably from those that assume the mantle to be isotropic. In particular, they do not have a pronounced LID of high velocity and have appreciably higher velocities in the vicinity of the low-velocity zone than the isotropic models. Evidence for a high-velocity layer at the top of the mantle must come from shorter period waves (Regan and Anderson, 1984).

It has long been known that isotropic models cannot simultaneously satisfy mantle Love wave and Rayleigh wave data. The Love wave–Rayleigh wave discrepancy, in fact, is the best evidence for widespread anisotropy of the upper 200 km or so of the mantle. It has been common practice in recent years to fit the Love wave and Rayleigh wave data separately and to take the difference in the resulting isotropic models as a measure of the anisotropy. This procedure is not valid since the equations of motion do not decouple in that way. In even the simplest departure from isotropy, transverse isotropy, five elastic constants must be determined to specify the velocities of propagation

of the quasi-longitudinal and two quasi-shear waves in all directions (see Chapter 15). This requires simultaneous inversion of Love wave and Rayleigh wave data including, if possible, higher modes.

Absorption and the LVZ

It is well known that elastic-wave velocities are independent of frequency only for a non-dissipative medium. In a real solid dispersion must accompany absorption. The effect is small when the seismic quality factor Q is large or unimportant if only a small range of frequencies is being considered. Even in these cases, however, the measured velocities or inferred elastic constants are not the true elastic properties but lie between the high-frequency and low-frequency limits or the so-called "unrelaxed" and "relaxed" moduli.

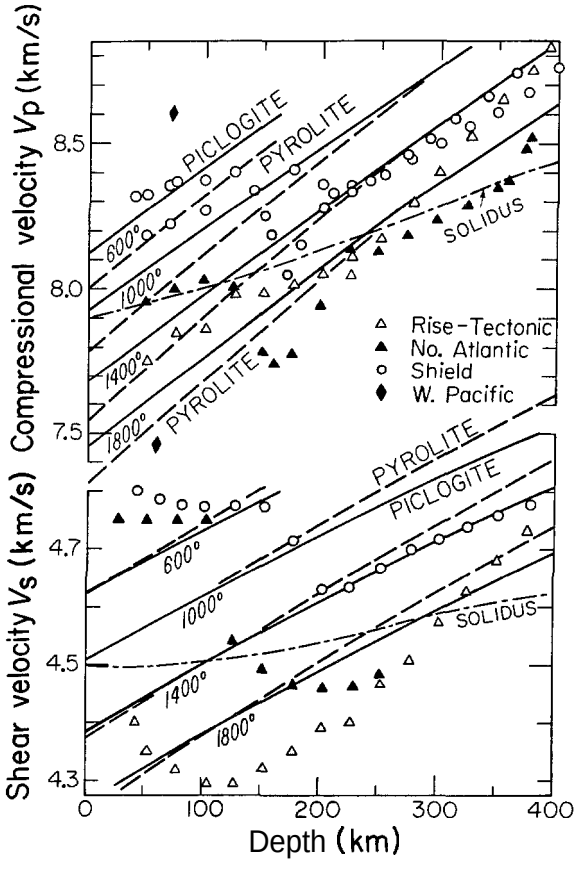

FIGURE 3-5
Compressional and shear velocities for two petrological models, pyrolite and piclogite, along various adiabats. The temperature ("C) are for zero pressure. The portions of the adiabats below the solidus curves are in the partial melt field. The seismic profiles are for two shields (Given and Helmberger, 1981; Walck, 1984), a tectonic-rise area (Grand and Helmberger, 1984a; Walck, 1984), and the North Atlantic (Grand and Helmberger, 1984b) region; two isolated points are Pacific Ocean data (Shimamura and others, 1977; after Anderson and Bass, 1984).

The magnitude of the effect depends on the nature of the absorption band and the value of Q. When comparing data taken over a wide frequency band, the effect of absorption can be considerable, especially considering the accuracy of present body-wave and free-oscillation data. Liu and others (1976) and Anderson and others (1977) showed that dispersion depends to first order on absorption in the seismic frequency band and derived a linear superposition model that gives a Q that is independent of frequency. They showed how to correct surface-wave and free-oscillation data for physical dispersion. Much of the early support for the existence of an upper-mantle low-velocity zone came from the inversion of normal-mode data uncorrected for physical dispersion due to absorption.

Anelasticity alone does not remove the necessity for a low-velocity zone, or a negative velocity gradient in the upper mantle. Allowance for anelastic dispersion (that is, frequency-dependent seismic velocities), however, makes it possible to reconcile normal-mode and body-wave models. The low upper-mantle velocities found by surface-wave and free-oscillation techniques were partially a result of low Q in the shallow mantle. Upper-mantle velocities are greater at short periods. The mechanism for low Q may involve dislocation relaxation or other subsolidus mechanisms.

The presence of physical dispersion complicates the problem of inferring chemistry and mineralogy by comparing seismic data with high-frequency ultrasonic data. This is less a problem if only the bulk modulus or seismic parameter @ is used.

Although seismic data alone are ambiguous regarding the presence or absence of partial melting, there are other constraints that can be brought to bear on the problem. Electrical conductivity, heat flow and the presence of volcanism often suggest the presence of partial melting in regions of the upper mantle where the seismic velocities are particularly low.

MINERALOGICAL MODELS OF 50–400 km DEPTH

Because of the intervention of partial melting and other relaxation phenomena in parts of the upper mantle, it is difficult to determine the mineralogy in this region. Figure 3-5 shows calculations for the seismic velocities for two different mineral assemblages. ***Pyrolite*** is a garnet peridotite composed mainly of olivine and orthopyroxene. ***Piclogite*** is a clinopyroxene- and garnet-rich aggregate with some olivine. Note the similarity in the calculated velocities. Below 200 km the seismic velocities under shields lie near the 1400" adiabat. Above 150 km the shield lithosphere is most consistent with cool olivine-rich material. The lower velocity regions have velocities so low that partial melting or some other high-temperature relaxation mechanism is implied. The adiabats falling below the solidus curves are predicted to fall in the partial melt field.

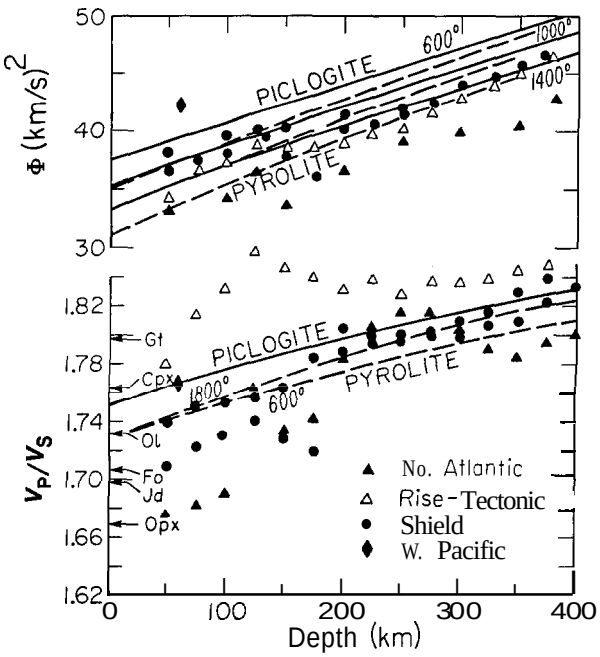

FIGURE **3-6**
Seismic parameter Φ and V_p/V_s for two petrological models and various seismic models. Symbols and sources are the same as in Figure 3-5. V_p/V_s ratios for various minerals are shown in the lower panel (after Anderson and Bass, 1984).

Figure 3-6 shows the calculated and observed bulk modulus Φ and V_p/V_s. The high V_p/V_s ratio for the rise-tectonic mantle is consistent with partial melting in the upper mantle under these regions.

The upper 200 km or so of the mantle is anisotropic. Deeper levels may be as well, but it is more difficult to detect anisotropy at depth. The anisotropy of the shallow mantle and the low density of olivine and orthopyroxene, combined with their refractory nature, compared to garnet-rich aggregates, are indirect arguments in favor of a peridotite **shallow** mantle. Kimberlite pipes contain fragments that appear to have come from below the continental lithosphere. Peridotites are the most common xenolith, but some pipes contain abundant eclogite. The eclogite could be samples of oceanic crust that have been subducted under the continental lithosphere, or trapped melts which froze before they made their way to the surface.

THE TRANSITION REGION

The transition region of the upper mantle, Bullen's region C, is generally defined as that part of the mantle between the 400-km and 650-km discontinuities. Sometimes the mantle below the bottom of the low-velocity zone (~190–250 km) is included. The 400-km discontinuity is often equated with the olivine-spinel phase change, considered as an equilibrium phase boundary in a homogeneous mantle, but there are serious problems with this interpretation. The seismic velocity jump is much smaller than predicted for this phase change (Duffy and Anderson, 1988). The orthopyroxene-garnet reaction leading to a garnet solid solution is also complete near this depth, possibly contributing to the rapid increase of velocity and density at the top of the transition region. For these reasons the 400-km discontinuity should not be referred to as the olivine-spinel phase change. If the discontinuity is as small as in recent seismic models, then a change in chemistry near 400 km is implied, or the olivine content of this part of the mantle is low.

In the classical mantle models of Harold Jeffreys and Beno Gutenberg, the velocity gradients between 400 and

TABLE 3-10
Measured and Estimated Properties of Mantle Minerals

Mineral	ρ (g/cm³)	V_p (km/s)	V_s (km/s)	V_p/V_s
Olivine ($Fa_{,,,}$)	3.37	8.31	4.80	1.73
β–Mg_2SiO_4	3.63	9.41	5.48	1.72
γ–Mg_2SiO_4	3.72	9.53	5.54	1.72
Orthopyroxene ($Fs_{.12}$)	3.31	7.87	4.70	1.67
Clinopyroxene ($Hd_{.12}$)	3.32	7.71	4.37	1.76
Jadeite	3.32	8.76	5.03	1.74
Garnet	3.68	9.02	5.00	1.80
Majorite	3.59	9.05*	5.06*	1.79*
Perovskite	4.15	10.13*	5.69*	1.78*
$(Mg_{.19}Fe_{.21})O$	4.10	8.61	5.01	1.72
Stishovite	4.29	11.92	7.16	1.66
Corundum	3.99	10.86	6.40	1.70

*Estimated.
Duffy and Anderson (1988), Weidner (1986).

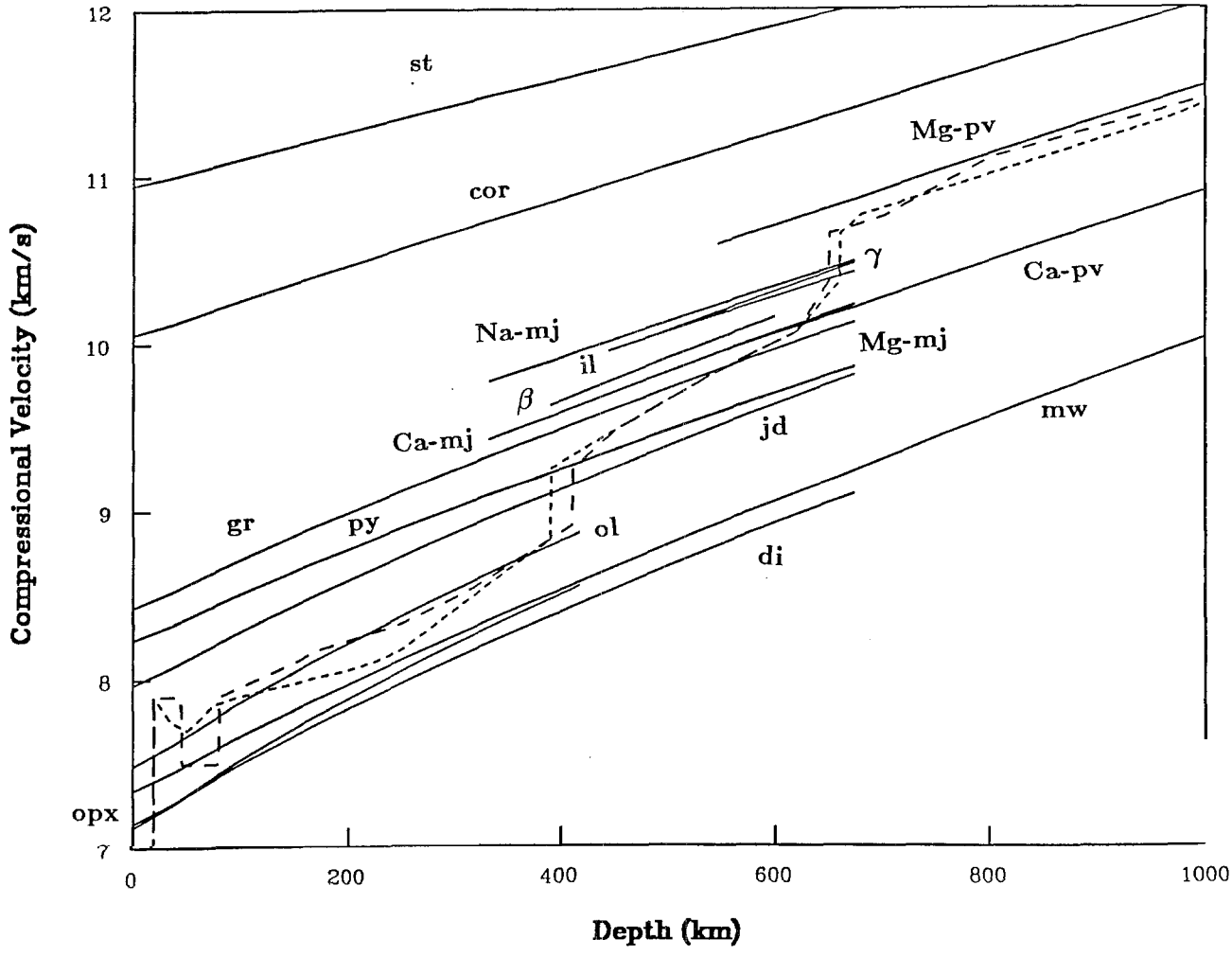

FIGURE 3-7
Calculated compressional velocity versus depth for various mantle minerals. "Majorite" (mj), "perovskite" (pv) and "ilmenite" (il) are structural, not mineralogical terms. The dashed lines are two recent representative seismic profiles (after Duffy and Anderson, 1988).

800 km were too high to be the result of self-compression; hence, it was called the transition region and was interpreted by Francis Birch as a region of phase changes. This region was later found to contain two major seismic discontinuities (Anderson and Toksöz, 1963; Niazi and Anderson, 1965; Johnson, 1967, 1969), one near 400 km and one near 650 km, which were initially attributed to the olivine-spinel and spinel–post-spinel phase changes, respectively, in an olivine-rich mantle (Anderson, 1967). (Properties of these and other deep mantle phases are listed in Table 3-10.) These phase changes are probably spread out over depth intervals of about 20 km and therefore result in diffuse seismic boundaries rather than sharp discontinuities. It was subsequently found that the 650-km discontinuity is a good reflector of seismic energy (Whitcomb and Anderson, 1970), requiring that its width be less than 4 km and that the large increase in elastic properties was not consistent with any phase change in olivine. There is also a high-gradient region below the discontinuity. The spinel–post-spinel transformation therefore is not an adequate explanation for the 650-km discontinuity. There appears to be no phase change in a chemically homogeneous mantle that has the requisite properties.

The velocity gradients between 400 and 650 km are higher than expected for a homogeneous self-compressed region. This region may represent the gradual conversion of diopside and jadeite to an Al_2O_3-poor garnet structure. In the presence of Al_2O_3-rich garnet, diopside is stable to much higher pressures than are calcium-poor pyroxenes.

In the transition zone the stable phases are garnet solid solution, β- and y-spinel and, possibly, jadeite. Garnet solid solution is composed of ordinary Al_2O_3-rich garnet and SiO_2-rich garnet (majorite). The extrapolated elastic properties of the spinel forms of olivine are higher than

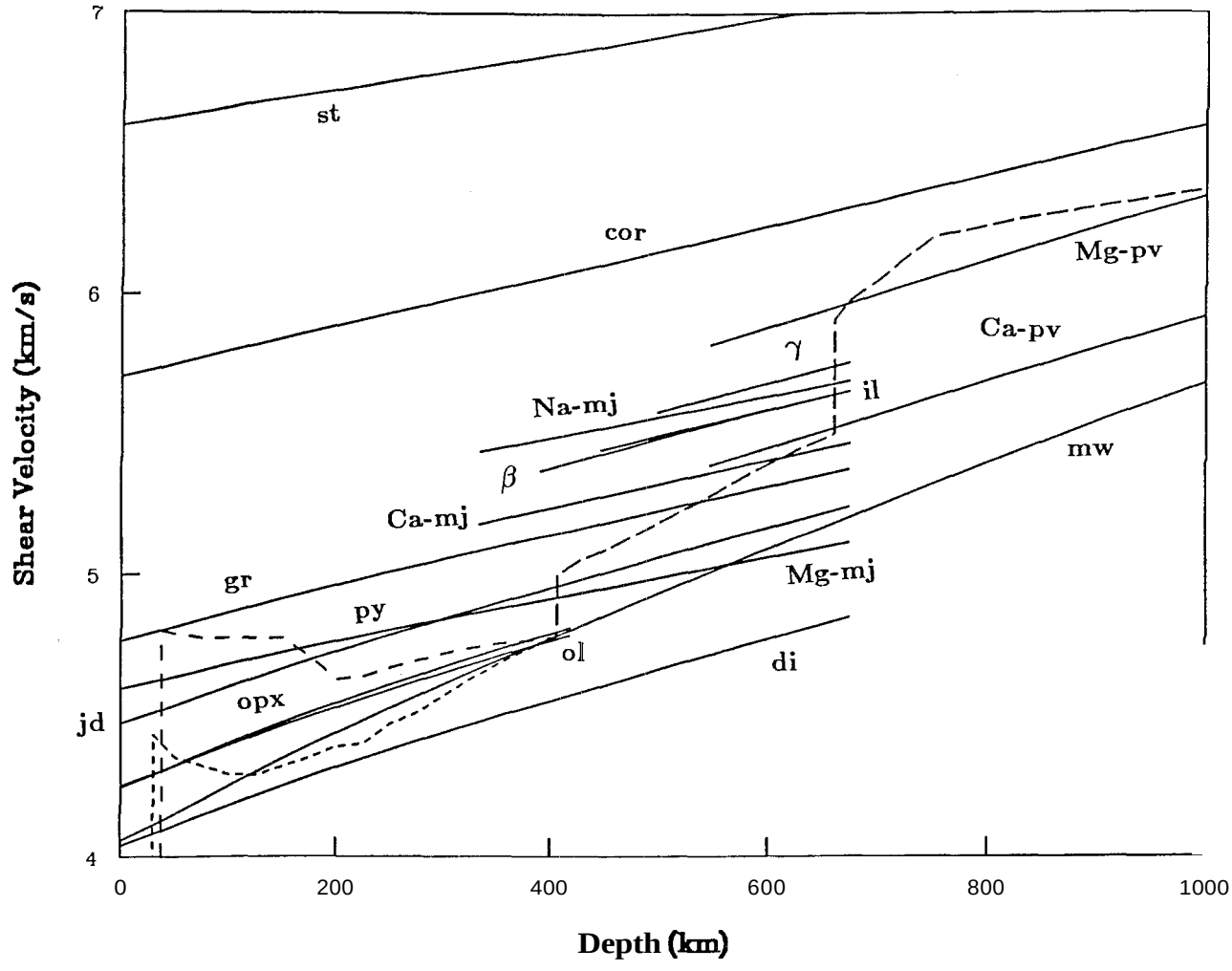

FIGURE 3-8
Same as Figure 3-7 but for the shear velocities (after Duffy and Anderson, 1988).

those observed (Figures 3-7 and 3-8). Pyroxenes in the garnet structure probably have elastic properties similar to ordinary garnet. $(Mg,Fe)SiO_3$ in the garnet structure is called "majorite"; I shall sometimes use this term to refer to any Al_2O_3-poor, SiO_2-rich garnet. The high velocity gradients throughout the transition zone imply a continuous change in chemistry or phase. Appreciable Al_2O_3-rich garnet is implied in order to match the velocities. A spread-out phase change involving clinopyroxene (diopside plus jadeite) transforming to Ca-rich majorite can explain the high velocity gradients. Detailed modeling (Bass and Anderson, 1984, Duffy and Anderson, 1988) suggests that olivine (in the β- and y-structures) is not the major constituent of the transition zone. The assemblage appears to be more eclogitic than pyrolite. The best fitting mineralogy contains less than 50 percent olivine.

The changes in elastic properties at the α–β phase boundary are large, but those at the β–γ phase change appear to be minor (Weidner and others, 1984). A small amount of olivine and orthopyroxene are adequate to explain the magnitude of the 400-km discontinuity by changing phase at this depth (Figures 3-9 and 3-10). Phase changes, however, in general, are smeared out over a considerable depth range and do not result in sharp discontinuities. Recent work suggests that the olivine–β-spinel transition may occur over a rather narrow pressure interval, but the predicted increase in seismic velocities is much greater than observed (Bina and Wood, 1986). Other calculations favor a spread-out α-to-β transition.

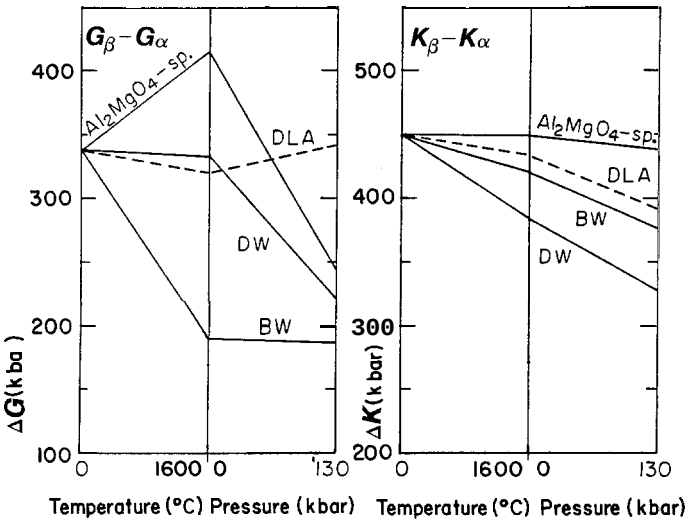

FIGURE 3-9
The 400-km seismic discontinuity is partially due to the α–β phase change in olivine. The amount of olivine implied by the size of the discontinuity depends on the as yet unmeasured pressure and temperature derivatives of the β-phase. The changes in rigidity (AG) and in bulk modulus (AK) associated with the phase change at zero pressure and low temperature are shown along the left axes. The changes with temperature and pressure are shown for various assumptions about the β-derivatives. If β-spinel has olivine-like derivatives, the AG and AK follow the dashed lines (DLA). The derivatives of Al_2MgO_4-spinel give the upper curves. Extreme values of the β-derivatives give the lines labeled DW and BW; in these two cases the AG and AK always decrease rightward and an olivine content of over 60 percent is allowed. For more normal values of the derivatives, less than 50 percent olivine is allowed. The conventional interpretation of the 400-km discontinuity is in terms of the olivine-spinel (β-phase) phase change in a peridotite mantle (olivine over 60 percent). These results suggest either a lower olivine content or a chemical transition to less olivine-rich material (as in an olivine eclogite).

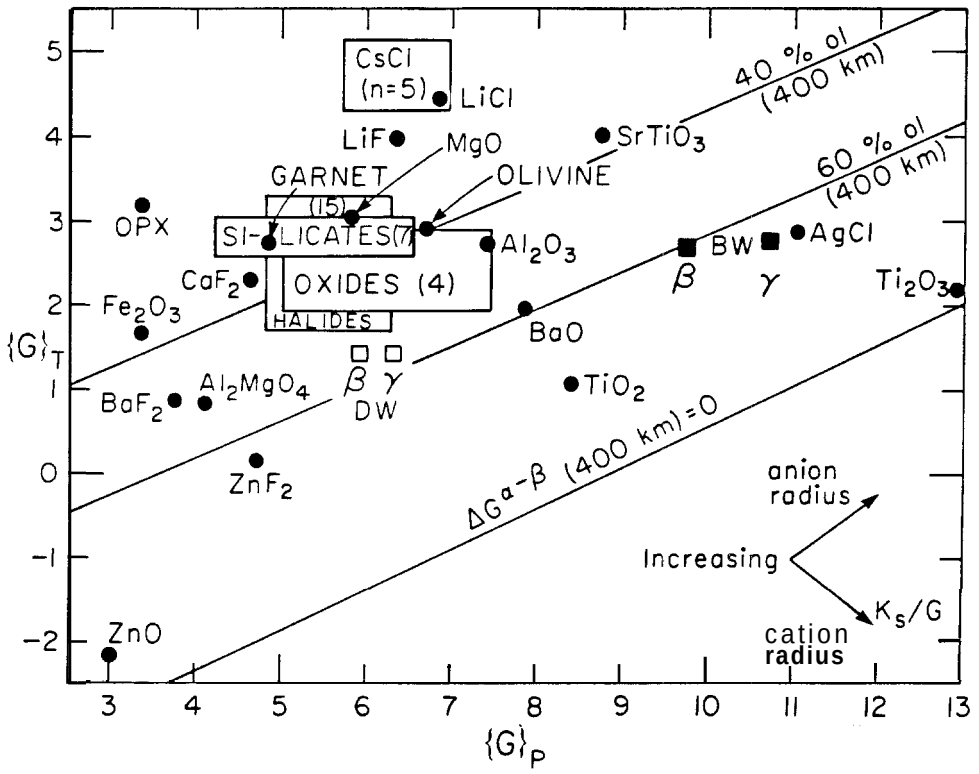

FIGURE 3-10
Normalized rigidity derivatives $\{G\}_T = (\partial \ln G/\partial \ln p)_T$ and $\{G\}_P = (\partial \ln G/\partial \ln \rho)_P$, for various minerals. The upper curve shows the $\{G\}_T$:$\{G\}_P$ relationship for silicates and oxides pertinent to the mantle. These values are consistent with an olivine content of 40 percent at 400 km based on the size of the seismic velocity jump at the 400-km discontinuity. The middle curve shows the parameter combinations required if the olivine content is 60 percent at 400 km. The lower curve assumes a zero rigidity increase at 400 km associated with the α–β phase change. BW and DW are parameters used by Bina and Wood (1986) and Weidner (1986).

General References

Anderson, D. L. (1982) Chemical composition and evolution of the mantle. In *High-pressure Research in Geophysics (S.* Akimoto and M. Manghnani, eds.), 301–318, D. Reidel, Dordrecht, Neth.

Condie, K. C. (1982) *Plate Tectonics and Crustal Evolution,* 2nd ed., Pergamon, New York, 310 pp.

Dziewonski, A. M. and D. L. Anderson (1981) Preliminary reference Earth model, *Phys. Earth Planet. Inter., 25,* 297–356.

Jacobs, J. A. (1975) *The Earth's Core,* Academic Press, London, 253 pp.

Levy, E. H. (1976) Kinematic reversal schemes for the geomagnetic dipole, *Astrophys. J., 171,* 635–642.

Melchior, P. (1986) *The Physics of the Earth's Core,* Pergamon, New York, 256 pp.

Parker, E. N. (1983) Magnetic fields in the cosmos, *Sci. Am., 249,* 44–54.

Ringwood, A. E. (1979) *Origin of the Earth and Moon,* Springer-Verlag, New York, 295 pp.

Taylor, S. R. (1982) *Planetary Science, a Lunar Perspective,* Lunar and Planetary Institute, Houston, 482 pp.

Taylor, S. R. and S. M. McLennan (1985) *The Continental Crust: Its Composition and Evolution,* Blackwell, London.

References

Anderson, D. L. (1966) Recent evidence concerning the structure and composition of the Earth's mantle. In *Physics and Chemistry of the Earth, 6,* 1–131, Pergamon, Oxford.

Anderson, D. L. (1967) Phase changes in the upper mantle, *Science,* 157, 1165–1173.

Anderson, D. L. (1979) The deep structure of continents, J. *Geophys. Res., 84,* 7555–7560.

Anderson, D. L. and J. D. Bass (1984) Mineralogy and composition of the upper mantle, *Geophys. Res. Lett., 11,* 637–640.

Anderson, D. L. and A. M. Dziewonski (1982) Upper mantle anisotropy: Evidence from free oscillations, *Geophys. Jow. Roy. Astr. Soc., 69,* 383–404.

Anderson, D. L., H. Kanamori, R. S. Hart and H. P. Liu (1977) The Earth as a seismic absorption band, *Science, 196,* 1104–1106.

Anderson, D. L. and C. G. Sammis (1970) Partial melting in the upper mantle, *Phys. Earth Planet. Inter., 3,* 41–50.

Anderson, D. L. and M. N. Toksoz (1963) Upper mantle structure from Love waves, *Jour. Geophys. Res., 68,* 3483–3500.

Babuska, V. (1972) Elasticity and anisotropy of dunite and bronzitite, *J. Geophys. Res., 77,* 6955–6965.

Bamford, D. (1977) P_n velocity anisotropy in a continental upper mantle, *Geophys. J.R. Astron. Soc., 49,* 29–48.

Bass, J. D. and D. L. Anderson (1984) *Geophys. Res. Lett., 11,* 237–240.

Bina, C. and B. Wood (1986) *Nature, 324,* 449.

Christensen, N. I. and J. N. Lundquist (1982) Pyroxene orientation within the upper mantle, *Geol. Soc. Amer. Bull., 93,* 279–288.

Christensen, N. I. and J. D. Smewing (1981) Geology and seismic structure of the northern section of the Oman ophiolite, *J. Geophys. Res., 86,* 2545–2555.

Clark, S. P., Jr. (1966) *Handbook of Physical Constants.* Geol. Soc. Amer. Mem. 97,587 pp.

Condie, K. L. (1982) *Plate Tectonics and Crustal Evolution,* 2nd ed., Pergamon, New York, 310 pp.

Drummond, B., K. Muirhead and A. L. Hales (1982) *Geophys. J. R. Astr. Soc., 70,* 67–77.

Duffy, T. and D. L. Anderson (1988) in press, *J. Geophys. Res.*

Dziewonski, A. M. and D. L. Anderson (1981) Preliminary reference Earth model, Phys. Earth Planet. Inter., 25, 297–356.

Forsyth, D. W. (1975) The early structural evolution and anisotropy of the oceanic upper mantle, *Geophys. J.R. Astron. Soc., 43,* 103–162.

Fuchs, K. (1977) Seismic anisotropy of the subcrustal lithosphere as evidence for dynamical processes in the upper mantle, *Geophys. J.R. Astron. Soc., 49,* 167–179.

Given, J. and D. Helmberger (1981) J. *Geophys. Res., 85,* 7183–7194.

Grand, S. and D. Helmberger (1984a) *Geophys. J.R.A.S., 76,* 399–438.

Grand, S. and D. Helmberger (1984b) J. *Geophys. Res., 88,* 801–804.

Gutenberg, B. (1959) *Physics of the Earth's Interior,* Academic Press, New York, 240 pp.

Hales, A. L., K. Muirhead and J. Rynn (1980) *Technophysics, 63,* 309–348.

Hart, R., D. L. Anderson and H. Kanamori (1976) The effect of attenuation on gross Earth models, *Earth and Planet. Sci. Lett., 32,* 25–34.

Isacks, B. and P. Molnar (1971) Distribution of stresses in the descending lithosphere from a global survey of focal-mechanism solutions of mantle earthquakes, *Rev. Geophys. Space Phys., 9,* 103–174.

Johnson, L. R. (1969) *Bull. Seis. Soc. Amer., 59,* 973–1008.

Johnson, L. R. (1967) Array measurements of P velocities in the upper mantle, *J. Geophys. Res., 72,* 6309–6325.

Jordan, T. H. (1979) In *The Mantle Sample* (F. R. Boyd and H. O. A. Meyer, eds.), American Geophysical Union, Washington, D.C.

Jordan, T. H. and L. N. Frazer (1975) Crustal and upper mantle structure from Sp phases, J. *Geophys. Res., 80,* 1504–1518.

Lehmann, I. (1961) S and the structure of the upper mantle, *Geophys. J. Roy. Astron. Soc., 4,* 124–138.

Leven, J. H., I. Jackson and A. Ringwood (1981) Upper mantle seismic anisotropy and lithospheric decoupling, *Nature, 289,* 234–239.

Liu, H. P., D. L. Anderson and H. Kanamori (1976) Velocity dispersion due to anelasticity; implications for seismology and mantle composition, *Geophys. J.R. Astron. Soc., 47,* 41–58.

Manghnani, M. et al. (1974) ***J. Geophys. Res., 79,*** 5427.

Morris, G. B., R. W. Raitt and G. G. Shor (1969) Velocity anisotropy and delay-time maps of the mantle near Hawaii, ***J. Geophys. Res., 74,*** 4300–4316.

Morse, S. A. (1986) ***Earth Planet. Sci. Lett., 81,*** 118–126.

Nataf, H.-C., I. Nakanishi and D. L. Anderson (1986) Measurements of mantle wave velocities and inversion for lateral heterogeneities and anisotropy, Part III. Inversion, ***J. Geophys. Res., 91,*** 7261–7307.

Niazi, M. (1969) Use of source arrays in studies of regional structure, ***Bull. Seismol. Soc. Amer., 59,*** 1631–1643.

Niazi, M. and D. L. Anderson (1965) Upper mantle structure of western North America from apparent velocities of P waves, ***Jour. Geophys. Res., 70,*** 4633–4640.

O'Hara, M. J. (1968) The bearing of phase equilibria studies in synthetic and natural systems on the origin and evolution of basic and ultrabasic rocks, ***Earth Sci. Rev., 4,*** 69–133.

Regan, J. and D. L. Anderson (1984) Anisotropic models of the upper mantle, ***Phys. Earth and Planet. Int., 35,*** 227–263.

Ringwood, A. E. (1975) ***Composition and Petrology of the Earth's Mantle,*** McGraw-Hill, New York, 618 pp.

Sacks, I. S., J. A. Snoke and E. S. Husebye (1977) Lithospheric thickness beneath the Baltic Shield, ***Carnegie Inst. Yearb., 76,*** 805–813.

Salisbury, M. and N. I. Christensen (1978) The seismic velocity structure of a traverse through the Bay of Islands ophiolite complex, Newfoundland, an exposure of oceanic crust and upper mantle, ***J. Geophys. Res., 83,*** 805–817.

Shimamura, H., T. Asada and M. Kumazawa (1977) ***Nature, 269,*** 680–682.

Sumino, Y. and 0 . L. Anderson (1984) Elastic constants of minerals. In ***Handbook of Physical Properties of Rocks,*** v. 3 (R. S. Carmichael, ed.), 39–138, CRC Press, Boca Raton, Florida.

Taylor, S. R. and S. M. McLennan (1985) ***The Continental Crust: Its Composition and Evolution,*** Blackwell, London.

Walck, M. (1984) ***Geophys. J.R.A.S. 76,*** 697–723.

Weidner, ***D.*** J. (1986) in ***Chemistry and Physics of Terrestrial Planets,*** Ed. S. K Saxena, Springer-Verlag, New York, 405 pp.

Weidner, D. J., H. Sawamoto, S. Sasaki and M. Kumazawa (1984) Single-crystal elastic properties of the spinel phase of Mg_2SiO_4, ***J. Geophys. Res., 89,*** 7852–7860.

Whitcomb, J. H. and D. L. Anderson (1970) Reflection of P'P' seismic waves from discontinuities in the mantle, ***J. Geophys. Res., 75,*** 5713–5728.